FOREX Publication
Open Access | Rapid and quality publishing

International Journal of
Electrical and Electronics Research (IJEER)
Research Article | Volume 12, Issue 2 | Pages 567-574 | e-ISSN: 2347-470X

Capacity Optimization of an Isolated Renewable Energy Microgrid Using an Improved Gray Wolf Algorithm

Jia Lu[1,2*], Fei Lu Siaw[1], Tzer Hwai Gilbert Thio[1] and Junjie Wang[3]

[1]Centre for Sustainability in Advanced Electrical and Electronic Systems (CSAEES), Faculty of Engineering, Built Environment and Information Technology, SEGi University, 47810 Petaling Jaya, Selangor, Malaysia; lujia445884870@163.com
[2]Department of Electronic Engineering, Taiyuan Institute of Technology, 030008, Taiyuan, Shanxi, China
[3]Department of Production and Environmental Protection, China Huaneng Group CO., Ltd. Shandong Branch. 250014 Jinan, Shandong, China

***Correspondence:** Jia Lu; *lujia445884870@163.com*

ABSTRACT- To achieve the goal of allocating the generation capacity of isolated renewable energy system microgrids in a stable, economical, and clean manner, an optimization model considering economic costs, environmental protection, and power supply reliability was established. Compared with the normalization of fixed weight coefficients, a dynamic adaptive parameter method was used in this study to balance the weights of economic, environmental, and stability factors in the objective function. The Levy Flight Strategy, Golden Sine Strategy, and Dynamic Inverse Learning Strategy were embedded to increase algorithm performance for optimization and simulation to address issues such as local optima, slow convergence speed, and lack of diversity commonly associated with traditional Grey Wolf Optimization algorithm. The case analysis shows that the Improved Grey Wolf Optimization algorithm effectively reduces the economic cost of microgrids, enhances environmental performance, and improves system reliability.

Keywords: Adaptive weights, Capacity optimization, Isolated renewable energy system (IRES), Improved gray wolf algorithm, Operational management strategy.

ARTICLE INFORMATION

Author(s): Jia Lu, Fei Lu Siaw, Tzer Hwai Gilbert Thio and Junjie Wang;

Received: 14/03/2024; **Accepted**: 20/05/2024; **Published**: 10/06/2024;
e-ISSN: 2347-470X;
Paper Id: IJEER 1403-19;
Citation: 10.37391/ijeer-120231
Webpage-link:
https://ijeer.forexjournal.co.in/archive/volume-12/ijeer-120231.html

Publisher's Note: FOREX Publication stays neutral with regard to Jurisdictional claims in Published maps and institutional affiliations.

1. INTRODUCTION

Global Electricity Review 2023 reveals a 15-20% growth rate for wind and solar energy sources over a decade [1]. Nevertheless, the effectiveness of these sustainable sources is inherently limited by their unpredictable nature and environmental variables, leading to significant fluctuations in energy production levels. Introducing hybrid renewable energy systems (HRES) has emerged as a necessary solution to counteract the instability observed in single-energy configurations. These hybrid systems amalgamate wind, solar, diesel, and storage elements, facilitating a cost-effective and consistent supply of electricity supply.

To construct a robust optimization model that addresses economic, environmental, and reliability considerations, it is essential to integrate key factors and constraints: The economic aspect often involves fixed and operational maintenance costs, which are determined by some factors such as initial capital outlay, ongoing maintenance expenses, and costs associated with component replacement [2; 3]. Environmental considerations are gauged by the reduction in emissions of harmful gases [4] and the increase in the adoption rate of renewable energy [4-7]. Meanwhile, reliability metrics focus on enhancing the system's self-balancing capabilities [8; 9] and minimizing the frequency of load-shedding events ([10-14]. Currently, capacity optimization techniques are broadly divided into two types. One employs Pareto front optimization, which harmonizes various objective functions such as economic factors, environmental impacts, and system reliability to derive optimal Pareto solutions. The alternative approach involves amalgamating numerous objective functions into a singular cohesive objective function through the allocation of distinct weights. Building on the previews of normalizing multiple targets with fixed weight coefficients, an adaptive weighting coefficient technique is introduced to correct the limitations associated with subjectively assigned fixed weights in the normalization process.

To achieve more precise optimal outcomes, various metaheuristic algorithms have been employed to address the objective function effectively. Sawle, et al. (2017) applied genetic algorithms and particle swarm optimization techniques to minimize the energy cost, aiming to enhance reliability, maximize renewable energy utilization, and reduce emissions and penalty costs. Different studies have implemented the Whale Optimization Algorithm (WOA) across various Hybrid Renewable Energy Systems (HRES) to optimize system capacity, ensuring adequate power supply at minimal cost for load demands [10; 16-18]. It was demonstrated that WOA

FOREX Publication
Open Access | Rapid and quality publishing
International Journal of Electrical and Electronics Research (IJEER)
Research Article | Volume 12, Issue 2 | Pages 567-574 | e-ISSN: 2347-470X

outperformed PSO in aspects of reliability, convergence speed, and accuracy. Another study introduced a design for a photovoltaic/diesel/battery system, need to minimize the annual total cost by employing the Grey Wolf Optimization (GWO) algorithm [19]. During the latter phases of maturation, the algorithm may confront challenges such as local convergence or premature convergence arising from a limited diversity within the populace. With the escalation of complexity in hybrid systems, traditional methodologies are progressively susceptible to being trapped in local optima [20; 21]. Aim at the defects of GWO, which is prone to premature convergence, low performance, and low accuracy in solving multi-modal complex problems, Yan(2020) proposed the chaotic Gray Wolf optimization algorithm from the aspect of GWO search mechanism, which is very competitive in training neural networks. It is an excellent algorithm that can deal with single-mode and multi-mode problems well, but its defects are also obvious. Through the simulation results on fixed-dimension multi-mode problems, we can see that the optimization performance of this algorithm is not ideal for fixed-dimension multi-mode problems. In the capacity optimization of independent micronets, Tent chaotic mapping, nonlinear convergence factor, and Cauchy mutation operator are adopted to improve the precocious performance of the Grey Wolf algorithm in the late stage of evolution. However, due to the relatively simple construction of the optimization target model, it only involves minimizing the cost of economic factors [23]. It does not fully reflect the complexity of practical applications. The article employs dynamic neighbourhood search technology to enhance the algorithm's ability to search for and distinguish multiple local optimal solutions. By considering multiple optimization factors such as cost, environmental impact, and system reliability, the practicality and versatility of the algorithm have been strengthened.

The distribution of chapters is structured as follows: the introductory section provides an overview, the subsequent section elaborates on the mathematical formulation of optimization, the Improved Grey Wolf Optimization Algorithm (IGWO) is expounded upon in *Sections 3*, optimization results are scrutinized and deliberated in *Section 4*, *Section 5* encapsulates the conclusions and prospects for future research.

2. MATHEMATICAL FORMULATION OF OPTIMIZATION

2.1 System Components Mathematical Modeling

The independent hybrid new energy system (HRES) discussed in this study is a self-sufficient electrical system that functions autonomously without reliance on the conventional power grid. The research highlights a HRES design that integrates the operation of a wind turbine, diesel generator, solar photovoltaic system, and storage battery in a collaborative manner.

2.1.1 Wind turbine (WT) mathematic modelling

The analysis of WT encompasses various factors, such as wind velocity, direction, energy density, atmospheric density, and selected turbine diameter. Among these factors, wind speed emerges as the paramount element. [15; 24-26]. The output power can calculate according to *equation (1):*

$$P_{wt}(t)=\begin{cases}0 & \mathrm{v}(t)\le v_i, v(t)\ge v_o\\ P_{wt-n}\cdot\frac{v(t)-v_i}{v_n-v_i} & v_i\le v(t)\le v_n\\ P_{wt-n} & v_n\le v(t)\le v_o\end{cases} \quad (1)$$

where, $P_{wt}(t)$ is the output power of WT; v_i represents the cut-in speed; set at 2.5 m/s; v_o is the cut-out speed, set at 18 m/s, v_n is the rated speed, set at 12 m/s; v(t) is the wind speed; $P_{wt\text{-}n}$ is the rated power.

2.1.2 PV mathematic modeling

The performance of a photovoltaic system is impacted by various factors, with temperature and light intensity being identified as the most crucial determinants of the system's output power. [27; 28]. The output power can be calculated by *equation (2):*

$$P_{pv}(t)=P_{pv-n}\cdot\frac{E_{ac}}{E_{STC}}\left[1+k_{pv}\left(T(t)-T_{STC}+30\frac{E_{ac}}{E_{STC}}\right)\right] \quad (2)$$

where, $P_{pv}(t)$ denotes output power (kW); $P_{pv\text{-}n}$ is the rated power at standard test condition (T_{STC} = 25℃, E_{STC}= 1000 W/m^2); k_{pv} is the temperature coefficient, set at -0.47%/℃; T(t) denotes ambient temperature (℃); E_{ac} is the sunlight irradiance (W/m^2).

2.1.3 Diesel generator mathematic modeling

The model used in this research to elucidate the relationship between diesel fuel consumption and the electrical power generated is expressed by *equation (3)* [4; 29-31]:

$$F_{\mathrm{dg}}(t)=\lambda_a\cdot P_{\mathrm{dg}-n}+\lambda_b\cdot P_{\mathrm{dg}}(t) \quad (3)$$

where, the fuel consumption ($F_{dg}(t)$) is determined by the power output ($P_{dg}(t)$) and the rated power ($P_{dg\text{-}n}$). Additionally, the fuel intercept coefficient (λ_a) and curve slope coefficient (λ_b) are denoted as 0.2461 and 0.08415 respectively, measured in L/kW.

2.1.4 Energy storage battery mathematic modeling

The evaluation of the storage battery's condition plays a pivotal role in assessing its efficiency and and capacity. This assessment hinges on the state of charge (SOC), a metric that takes into account the entirety of charging and discharging operations [24; 32-34]. the mathematical representation of SOC can elucidate through *equation (4):*

$$SOC(t)=\begin{cases}(1-\varepsilon)SOC(t-1)+\frac{P_c(t)\eta_c}{E_{STC}}\\ (1-\varepsilon)SOC(t-1)-\frac{P_{dis}(t)/\eta_{dis}}{E_{STC}}\end{cases} \quad (4)$$

where, SOC represents the status of the battery; the self-discharge coefficient, denoted as ε, is established at a value of 2%; $P_{dis}(t)$ denotes the discharging power and and $P_c(t)$ denotes charging power (kW); η_c and η_{dis} are the energy efficiency during charging and discharging, both 95%; E_{STC} is the rated battery capacity (kWh).

FOREX Publication
Open Access | Rapid and quality publishing
International Journal of Electrical and Electronics Research (IJEER)
Research Article | Volume 12, Issue 2 | Pages 567-574 | e-ISSN: 2347-470X

2.2 Optimal Objective

2.2.1 Mitigation of cost

The overall cost consists of several parts as shown in *equation (5)*

$$C_E = min(C_{pi} + C_{\text{om}} + C_r + C_f) = min\left\{\sum_{i=1}^{N}\left[\frac{r_i(1+r_i)^{d_i}}{(1+r_i)^{d_i-1}}\cdot \frac{f(i)\cdot P(i)}{365 d_i}\right] + \sum_{i=1}^{N}\sum_{t=1}^{24}[c_{om-i}\cdot P_i(t)] + \sum_{i=1}^{N}\sum_{t=1}^{24}[c_{r-i}\cdot P_i(t)] + c_{die}\cdot\sum_{t=1}^{24}\left[\lambda_a P_{dg-n} + \lambda_b P_{dg}(t)\right]\right\} \quad (5)$$

where, C_E is economic function; C_{pi} is the purchasing cost; C_{om} is the operation and maintenance cost (O&M cost); C_r is the replacement cost; C_f is the fuel cost of diesel; r_i is the discount rate of the i^{th} equipment, f(i) is the unit cost of i^{th} equipment, the unit is yuan/kW; d_i is the lifecycle of the i^{th} equipment (year); $P_i(t)$ is the output power of the i^{th} equipment at time t; P(i) is the maximum power of the i^{th} equipment (kW); c_{die} is the unit fuel cost, unit is yuan/L .

2.2.2 Reduction of emission

The objective function is chiefly expressed through emission levels of pollutants and control factors, as outlined in *equation (6)*.

C_{envir} is pollution abatement costs, β_k is the emission coefficient, set unit g/kW·h; α_k is the control standard coefficient; k is the pollutant type. The parameters are shown in *table 1* [35].

$$C_{envir}(t) = \sum_{k=1}^{3}\left[\alpha_k \beta_k P_{dg}(t)\right] \quad (6)$$

Table 1. Pollution factors

Pollutant type	α_k: Pollution control standard factor	β_k: Pollutant discharge factor (g/kWh)
CO_2	0.21	649
SO_2	14.842	0.206
NO_x	62.964	9.89

2.2.3 Reliability index

The power deviation rate including load shedding power and energy waste power is utilized to assess the power supply reliability [36], as represented in *equation (7):*

$$C_{reliability}(t) = c_w P_{cutp}(t) + c_v P_{cutl}(t) \quad (7)$$

where, $C_{reliability}$ represents the penalty cost; c_w denotes the penalty unit price for overpower; c_v signifies the price for power shortage; $P_{cutp}(t)$ is the energy waste power at time t; $P_{cutl}(t)$ indicates the load shedding power at time t.

2.2.4 Normalized objective function

The weighted objective function method assigns weights to economic, environmental, and reliability factors, multiplies them, and aggregates them into a scalar objective function[36-39]. However, the subjective weight selection can greatly influence optimization outcomes. This study introduces adaptive weighting as a solution. The adaptive weight technique modifies the weights of the objective function iteratively according to the obtained optimization outcomes and specific problem attributes. The planning model is detailed in Equations (4-7) [40]

$$C = \sum_{t=1}^{24}\beta_1(t)\cdot\frac{C_{invest}}{24} + \beta_1(t)\cdot C_{opera} + \beta_1(t)\cdot C_{replace} + \beta_1(t)\cdot C_{fuel} + \sum_{t=1}^{24}[\beta_2(t)\cdot C_{envir}(t)] + \sum_{t=1}^{24}[\beta_3(t)\cdot C_{reli}(t)] \quad (8)$$

$$\beta_1(t) + \beta_2(t) + \beta_3(t) = 1 \quad (9)$$

$$\begin{cases}\beta_2(t) = \frac{C_{envir}(t)}{max[C_{envir}(1), C_{envir}(2), \cdots, C_{envir}(24)]}\cdot 0.7 \\ \beta_3(t) = \frac{C_{reli}(t)}{max[C_{reli}(1), C_{reli}(2), \cdots, C_{reli}(24)]}\cdot 0.7\end{cases} \quad (10)$$

$$\begin{cases}\beta_2(t) \in [0.1, 0.35] \\ \beta_3(t) \in [0.1, 0.35]\end{cases} \quad (11)$$

where, $\beta_1(t)$, $\beta_2(t)$ and $\beta_3(t)$ indicates cost, emission, and reliability index weight at time t.

2.2 Design constraints

Equality and inequality constraints are shown in *equation (12-15)* [4; 12; 14; 41; 42]:

$$P_{wt}(t) + P_{pv}(t) + P_{bat}(t) + P_{dg}(t) + P_{cutp}(t) = P_{load}(t) + P_{cutl}(t) \quad (12)$$

$$P_{bat}(t) = P_{dis}(t) - P_{ch}(t) \quad (13)$$

$$\begin{cases} P_{ch}^{\min} \le P_{ch}(t) \le P_{ch}^{\max} \\ P_{dis}^{\min} \le P_{dis}(t) \le P_{dis}^{\max} \\ P_{ch}^{\max} = P_{dis}^{\max} = \frac{1}{2}E_{bat} \\ SOC_{\min} \le SOC(t) \le SOC_{\max} \end{cases} \quad (14)$$

$$P_{dg}^{min} \le P_{dg}(t) \le P_{dg}^{max} \quad (15)$$

where, P_{ch}^{max} and P_{ch}^{min} represent the upper and lower charge power; P_{dis}^{min} and P_{dis}^{max} represent the lower and upper discharge power; SOC_{min} and SOC_{max} represent the lower and upper SOC value; P_{dg}^{max} and P_{dg}^{min} represent the diesel generator upper and lower output power.

3. IMPROVED GREY WOLF OPTIMIZATION

Mirjalili,et al.(2014) proposed the Grey Wolf Optimization (GWO) algorithm. The gray Wolf population's prey behavior was simulated to optimize mutual cooperation within the group. Due to the rapid decline of population diversity, the basic GWO algorithm often encounters the problems of prematurity and local convergence, which limits its further application in the field of engineering optimization. This paper adopt Levy Flight Strategy and Golden Sine Strategy to improve the global optimal character. The following are enhanced steps of IGWO:

Step-1: When seeking the prey, establish a dispersion model, generating a random variable A. when |A| ≤ 1, grey wolves

FOREX Publication
Open Access | Rapid and quality publishing
International Journal of Electrical and Electronics Research (IJEER)
Research Article | Volume 12, Issue 2 | Pages 567-574 | e-ISSN: 2347-470X

adopt a strategy of grouping together to enclose the prey. In contrast, when |A| > 1, individual grey wolves exhibit a behavior of distancing themselves from located prey to pursue more formidable targets. C is a stochastic variable within [0, 2], serving as a probabilistic factor influencing the weight assigned to the prey. Such stochasticity contributes to the modulation of the prey's influence on the spatial arrangement of the grey wolves during subsequent iterations. A and C expressions are as *equation (16-17)*:

$$A = 2a \cdot r_1 - a \tag{16}$$

$$C = 2r_2 \tag{17}$$

where, r_1 and r_2 are random value within [0, 1]; a is a convergence factor gradually decreasing from 2 to 0 during the iteration process.

Step-2: During the process of capturing, the grey wolves surround the prey, the mathematical model is as follows *equation (18-19):*

$$D = \left|C \cdot X_p(t) - X(t)\right| \tag{18}$$

$$X(t+1) = X_p(t) - A \cdot D \tag{19}$$

where, D is the distance between the prey and the individual grey wolf; X_p is the prey position; $X(t)$ is the individual grey wolf positions in *t-th* iterations.

Step-3: The wolf pack, led by the α, β, δ wolves, continuously approaches its prey, their positions are constantly changing until a successful hunt is achieved. This process can be represented by *equation (20-22):*

$$\begin{cases} D_\alpha(t) = |C_1 \cdot X_\alpha(t) - X(t)| \\ D_\beta(t) = \left|C_2 \cdot X_\beta(t) - X(t)\right| \\ D_\delta(t) = |C_3 \cdot X_\delta(t) - X(t)| \end{cases} \tag{20}$$

$$\begin{cases} X_\alpha'(t) = X_\alpha(t) - A_1 \cdot D_\alpha(t) \\ X_\beta'(t) = X_\beta(t) - A_2 \cdot D_\beta(t) \\ X_\delta'(t) = X_\delta(t) - A_3 \cdot D_\delta(t) \end{cases} \tag{21}$$

$$X(t+1) = \frac{X_\alpha'(t) + X_\beta'(t) + X_\delta'(t)}{3} \tag{22}$$

where, $D_\alpha(t)$, $D_\beta(t)$ and $D_\delta(t)$ are the spatial separations between α, β, δ wolves and individual wolf; $X_\alpha(t)$, $X_\beta(t)$ and $X_\delta(t)$ are the α, β, δ wolve positions at the *t-th* iteration; $X_\alpha'(t)$, $X_\beta'(t)$ and $X_\delta'(t)$ represent the individual positions affected by α, β, and δ wolves; The average of these three positions is considered to be the position of the individual wolf in subsequent iterations.

Step-4a: The Golden Sine Strategy not only involves the current location and the target location, but also controls the search step size by introducing an adjusted sinusoidal waveform, enabling the search process to be dynamically adjusted between exploration and exploitation, helps to accurately approach the global optimal solution for a known good region. The basic Sine Strategy expression is *equation (23-24),* the improved expression are as follows *equation (25-26):*

$$X_{\text{new}}(t) = X_{current}(t) + A(t) \times sin(\omega t) \times \left(X_{target}(t) - X_{current}(t)\right) \tag{23}$$

$$A(t) = A_0 \cdot e^{-\lambda t} \tag{24}$$

where, $X_{new}(t)$, $X_{current}(t)$, $X_{target}(t)$ denote the new position, current position, and target position of individual wolf; A is amplitude, ω is frequency, A_0 is initial amplitude, λ is attenuation coefficient.

$$X_{gold}(t) = X(t) \times |sin(R_1)| + R_2 \times sin(R_1) \times |x_1 X_{best}(t) - x_2 X(t)| \tag{21}$$

$$\begin{cases} x_1 = -\pi + (1-\tau) \cdot 2\pi \\ x_2 = -\pi + \tau \cdot 2\pi \end{cases} \tag{25}$$

$$\tau = \frac{\sqrt{5}-1}{2} \tag{26}$$

where, $X_{gold}(t)$, $X(t)$, $X_{best}(t)$ denote the new position, current position, and target position of individual wolf; τ is golden ration; x_1 and x_2 are angular variables introducing the properties of the golden ratio into the Angle adjustment, thus may optimize the diversity and efficiency of the search path; R_1 and R_2 denote stochastic variables within the range [0, 2π]; R_1 dictating magnitude of the individual forthcoming movement, R_2 determines the orientation of the next movement.

Step-4b: The Levy Flight Strategy helps the algorithm to perform a large range of jumps, jumping out of local optimal solutions. Its mathematical expression is as follows Equation (27-30):

$$X_{Levy}(t) = Levy(d) \cdot X_{best}(t) + \xi |X(t) - X_{best}(t) \cdot Levy(d)| \tag{27}$$

$$Levy(d) = 0.01 \times \frac{\sigma \cdot r_1}{|r_2|^{\frac{1}{\xi}}} \tag{28}$$

$$\sigma = \left\{ \frac{\Gamma(1+\xi) \cdot sin(\frac{\pi\xi}{2})}{\Gamma\left[\frac{(1+\xi)}{2}\right] \xi \cdot 2^{\frac{\xi-1}{2}}} \right\}^{\frac{1}{\xi}} \tag{29}$$

$$\Gamma(z) = \int_0^\infty t^{z-1} e^{-t} dt \tag{30}$$

Where, $X_{Levy}(t)$ evaluates the step array based on the dimensions provided (dim) which is scaling by 0.01 to control the step size in the solution space; d is the independent variable dimensionality, set 4; ξ is a constant, set 1.5; Γ is the gamma function. Scaling the random step size by calculating σ ensures that the step size has the correct statistical properties based on the selected beta value.

FOREX Publication
Open Access | Rapid and quality publishing
International Journal of Electrical and Electronics Research (IJEER)
Research Article | Volume 12, Issue 2 | Pages 567-574 | e-ISSN: 2347-470X

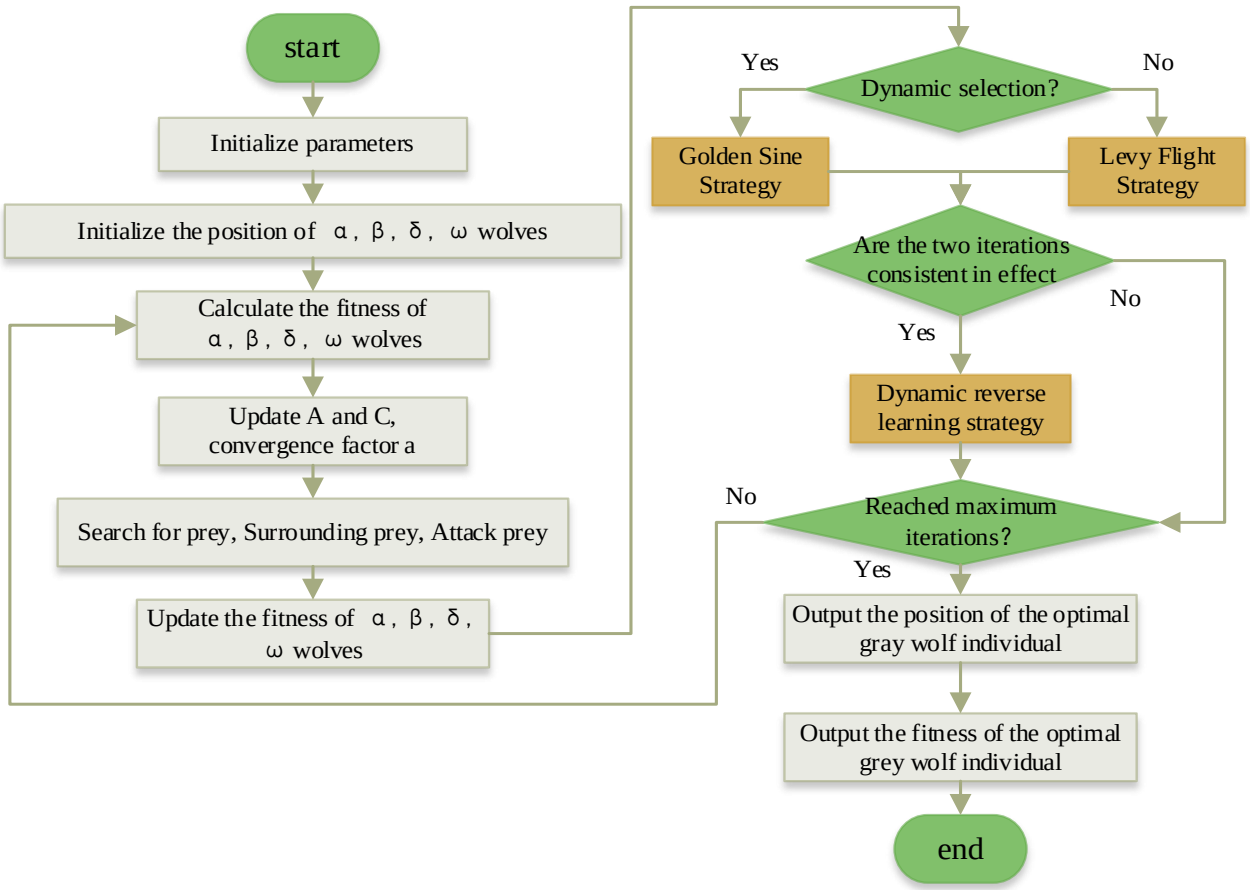

Figure 1. The IGWO algorithm flowchart

Step-5: The Dynamic Reverse Learning Strategy produces both the optimal individual and the reverse learning individual, subsequently choosing between the two based on their fitness values. A greedy strategy is used to select the optimal individual, as described by *equation (31)*:

$$X_{DOBL}(t) = r_3\{r_4[X_{LB} + X_{UB} - X_{best}(t)] - X_{best}(t)\} + X_{best}(t) \quad (31)$$

where, the position of each grey individual is adjusted through the dynamic reverse learning strategy at the t^{th} iteration, denoted as $X_{DOBL}(t)$; r_3 and r_4 represent randomly generated numbers within the range of 0 to 1; Moreover, X_{UB} and X_{LB} symbolize the upper and lower limits of the independent variable; ($X_{LB} + X_{UB}$-X_{Best}) denotes new positions and find potential better solutions by exploring symmetric points in the current solution space. The new location is generated by considering the boundary information, so that the algorithm can use the limit information of the whole search space to explore the opposite direction of the center of the solution space on the basis of the optimal solution.

The flowchart of IGWO algorithm is illustrated in *figure. 1*.

4. RESULTS AND DISCUSSION

The study selected the conventional daily load information originating from a community hospital situated in California, USA, to serve as the load data for the HRES microgrid. The scheduling timeframe encompasses T=24 hours, with a sampling interval of 1 hour. The expense and related cost factors of equipment are detailed in Table 2 [27].

Table 2. The expenses and related cost factors of the decentralized power source

Type	Unit	WT	PV	DG	BAT
Investment cost	10^4yuan·kW^{-1}	0.45	0.5	0.13	0.57
O&M cost	yuan·kW^{-1}	0.0354	0.0887	0.0257	0.0057
Replaced cost	10^4yuan·kW^{-1}	0	0	0.1	0.45
Lifetime	year	20	20	20	10

FOREX Publication
Open Access | Rapid and quality publishing
International Journal of Electrical and Electronics Research (IJEER)
Research Article | Volume 12, Issue 2 | Pages 567-574 | e-ISSN: 2347-470X

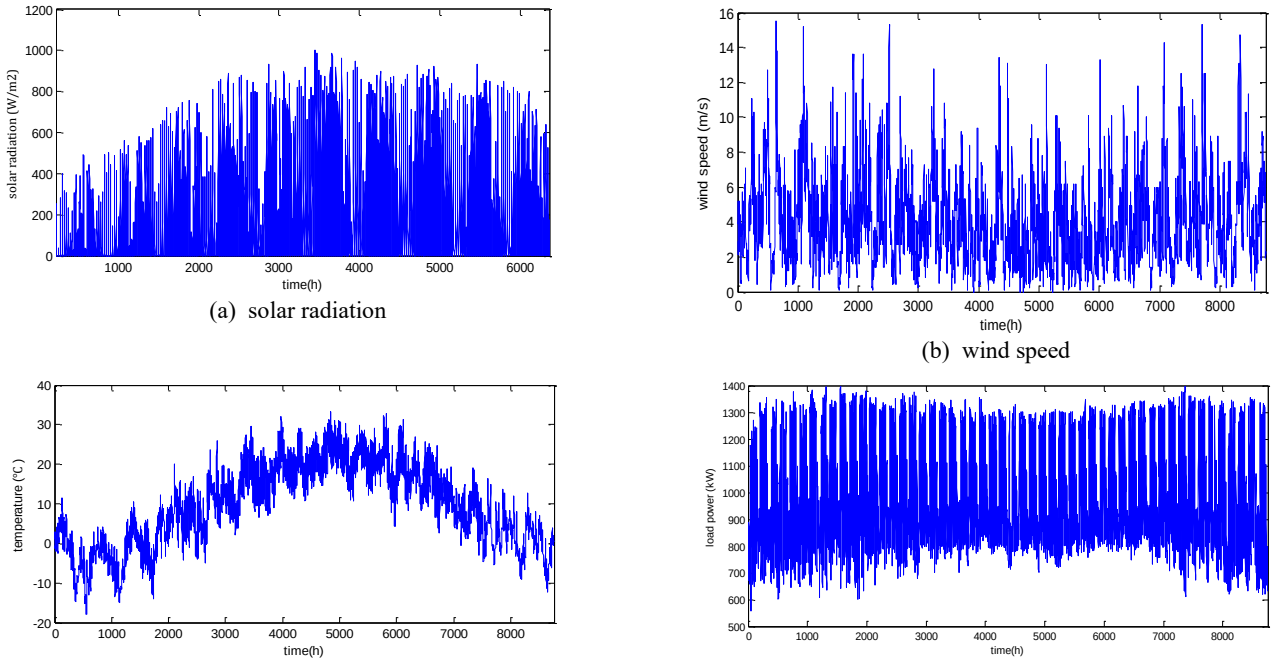

(a) solar radiation (b) wind speed (c) temperature (d) load power

Figure 2. Hourly profile of solar radiation, wind speed, temperature and load in a year

From *figure. 4*, the diagram shows the power balance of each component. The the storage battery SOC and output power are shown in *figure. 5*. The adaptive weight coefficient results are illustrated in *figure. 6*.

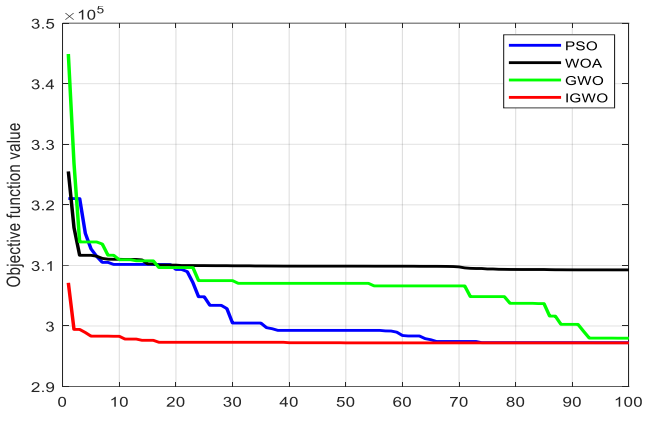

Figure 3. Comparison diagram of convergence process

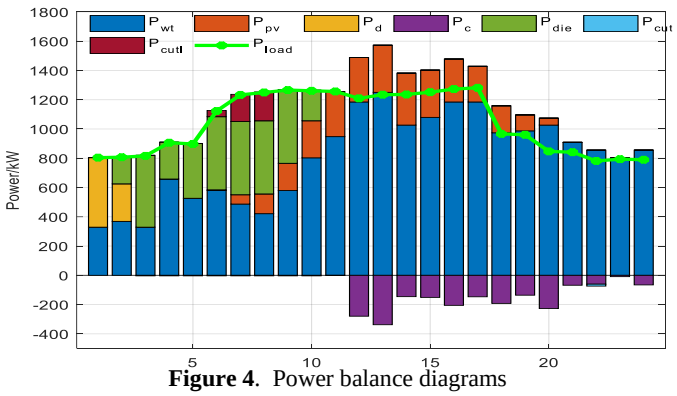

Figure 4. Power balance diagrams

In *figure. 3*, it can be observed that during the iterative process, the IGWO algorithm demonstrates superior convergence speed, with convergence curves displaying a consistent trend towards the optimal solution.

As illustrated in *table 3*, both PSO and IGWO algorithms reach the optimal solution at 297,212 in the 76th, and 50th iterations, IGWO significantly enhances convergence speed. *Table 4* shows the system components' unit capacity and optimized capacity.

Table 3. Convergent optimal solutions

algorithm	Optimal results（yuan）	Convergent number
PSO	297212	76
WOA	309265	80
GWO	297985	94
IGWO	297212	50

Table 4. Optimized equipment capacity

Type	Unit capacity (kW)	Capacity (kW)
WT	20	1206
PV	20	491
DG	10	695
BAT	10	1600

FOREX Publication
Open Access | Rapid and quality publishing
International Journal of Electrical and Electronics Research (IJEER)
Research Article | Volume 12, Issue 2 | Pages 567-574 | e-ISSN: 2347-470X

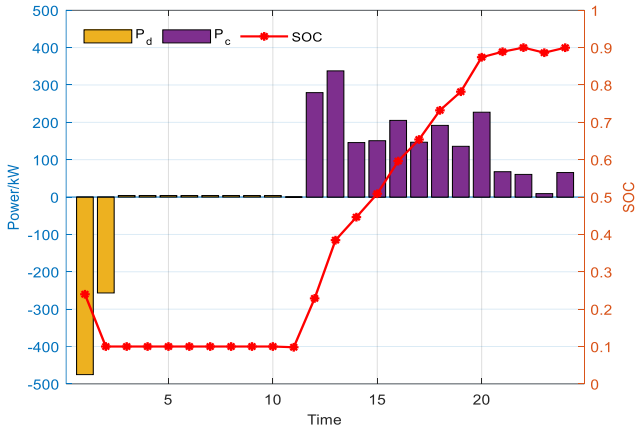

Figure 5. SOC status and output power of battery

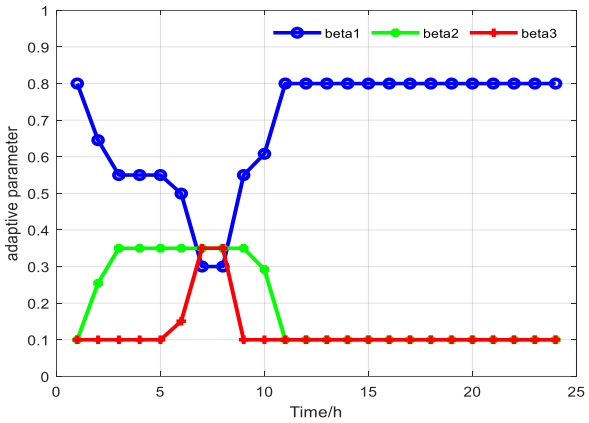

Figure 6. Dynamic adaptive parameters

These variations of adaptive weight coefficients indicate that the system automatically adjusts its emphasis on economy, environmental friendliness, and reliability during different periods to adapt to varying workloads and external conditions.

5. CONCLUSIONS AND PERSPECTIVES

The study explores the balance of economic, environmental friendliness, and reliability aspects of renewable energy system microgrids through the weighted objective function method. By introducing adaptive weighting, the subjectivity of weight selection is reduced. Using the Golden Sinusoidal strategy and the Levy Flight strategy effectively avoids local optima problems and accelerates the convergence speed of the algorithm. In subsequent iterations, the dynamic reverse learning strategy avoids stagnation, effectively preventing falling into local optima. Future research will add sensitivity analysis of adaptive coefficients, assessing the influence of varying weight scenarios on optimization outcomes, and consider adopting other improved technologies and renewable energy sources to meet heating and cooling needs, further promoting the sustainability of renewable energy systems. Additionally, the possibility of implementing more optimal algorithms will be explored.

REFERENCES

[1] Małgorzata Wiatros-Motyka. (2023). Global Electricity Review 2023. https://ember-climate.org/insights/research/global-electricity-review-2023/#supporting-material

[2] Chen J, Zhang W, Li J, *et al.* (2017). Optimal Sizing for Grid-tied Microgrids with Consideration of Joint Optimization of Planning and Operation. *IEEE Transactions on Sustainable Energy*, 9, 237-248.

[3] Guo L, Liu W, Jiao B, *et al.* (2014). Multi-objective stochastic optimal planning method for stand-alone microgrid system. *IET Generation Transmission & Distribution*, 8(7), 1263-1273.

[4] Kamal MM, Ashraf I, Fernandez E. (2023). Optimal energy management and capacity planning of renewable integrated rural microgrid. *Environmental Science and Pollution Research*, 30(44), 99176-99197.

[5] Bukar AL, Tan CW, Yiew LK, *et al.* (2020). A rule-based energy management scheme for long-term optimal capacity planning of grid-independent microgrid optimized by multi-objective grasshopper optimization algorithm. *Energy Conversion and Management*, 221, 113161-113183.

[6] Tang W, Liu Q, He P, *et al.* (2021). A Distributed Optimal Scheduling Method Based on Microgrid Cluster of Plug and Play. *IOP Conference Series. Earth and Environmental Science*, 701(1), 012058-012073.

[7] Tawfik M, Shehata AS, Hassan AA, *et al.* (2023). Renewable solar and wind energies on buildings for green ports in Egypt. *Environmental Science and Pollution Research* 30(16), 47602-47629.

[8] Akram U, Khalid M, Shafiq S. (2017). An Innovative Hybrid Wind-Solar and Battery-Supercapacitor Microgrid System—Development and Optimization. *IEEE Access*, 5, 25897-25912.

[9] Abbes D, Martinez A, Champenois G. (2014). Life cycle cost, embodied energy and loss of power supply probability for the optimal design of hybrid power systems. *Mathematics and Computers in Simulation*, 98, 46-62.

[10] Yahiaoui A, Tlemçani A. (2022). Superior performances strategies of different hybrid renewable energy systems configurations with energy storage units. *Wind Engineering*, 46(5), 1471-1486.

[11] Lorestani A, Gharehpetian GB, Nazari MH. (2019). Optimal sizing and techno-economic analysis of energy- and cost-efficient standalone multi-carrier microgrid. *Energy*, 178, 751-764.

[12] Javed MS, Ma T, Jurasz J, *et al.* (2020). Performance comparison of heuristic algorithms for optimization of hybrid off-grid renewable energy systems. *Energy*, 210, 118599-118618.

[13] Aeidapu MAHESH KSS. (2020). A genetic algorithm based improved optimal sizing strategy for solar-wind-battery hybrid system using energy filter algorithm. *Front. Energy*, 14(1), 139-151.

[14] Haddadian Nezhad E, Ebrahimi R, Ghanbari M. (2023). Fuzzy Multi-objective allocation of photovoltaic energy resources in unbalanced network using improved manta ray foraging optimization algorithm. *Expert Systems with Applications*, 234, 121048-121065.

[15] Sawle Y, Gupta SC, Bohre AK. (2017). Optimal sizing of standalone PV/Wind/Biomass hybrid energy system using GA and PSO optimization technique. *Energy Procedia*, 117, 690-698.

[16] Diab AAZ, Sultan HM, Kuznetsov ON. (2020). Optimal sizing of hybrid solar/wind/hydroelectric pumped storage energy system in Egypt based on different meta-heuristic techniques. *Environ Sci Pollut Res Int*, 27(26), 32318-32340.

[17] Sun H, Ebadi AG, Toughani M, *et al.* (2022). Designing framework of hybrid photovoltaic-biowaste energy system with hydrogen storage considering economic and technical indices using whale optimization algorithm. *Energy*, 238.

International Journal of Electrical and Electronics Research (IJEER)
Research Article | Volume 12, Issue 2 | Pages 567-574 | e-ISSN: 2347-470X

[18] Alturki FA, Awwad EM. (2021). Sizing and Cost Minimization of Standalone Hybrid WT/PV/Biomass/Pump-Hydro Storage-Based Energy Systems. *Energies*, 14(2), 489-509.

[19] Yahiaoui A, Fodhil F, Benmansour K, *et al.* (2017). Grey wolf optimizer for optimal design of hybrid renewable energy system PV-Diesel Generator-Battery: Application to the case of Djanet city of Algeria. *Solar Energy*, 158, 941-951.

[20] Baños R, Manzano-Agugliaro F, Montoya FG, *et al.* (2011). Optimization methods applied to renewable and sustainable energy: A review. *Renewable and Sustainable Energy Reviews*, 15(4), 1753-1766.

[21] Lian J, Zhang Y, Ma C, *et al.* (2019). A review on recent sizing methodologies of hybrid renewable energy systems. *Energy Conversion and Management*, 199, 112027-112050.

[22] Yan F. (2020). Improvement Research on the Grey Wolf Optimizer. (Doctor of Management), Harbin Engineering University,

[23] Zhao C, Wang B, Sun Z, *et al.* (2022). Optimal configuraiton optimization of island microgrid using Improved wolf optimizer algorithm. *Acta Energiae Solaris Sinica*, 43(01), 256-262.

[24] Liu C, Wang X, Wu X, *et al.* (2017). Economic scheduling model of microgrid considering the lifetime of batteries. *IET Generation, Transmission & Distribution*, 11(3), 759-767.

[25] Ma T, Yang H, Lu L, *et al.* (2014). Technical feasibility study on a standalone hybrid solar-wind system with pumped hydro storage for a remote island in Hong Kong. *Renewable Energy*, 69, 7-15.

[26] Sfikas EE, Katsigiannis YA, Georgilakis PS. (2015). Simultaneous capacity optimization of distributed generation and storage in medium voltage microgrids. *International Journal of Electrical Power & Energy Systems*, 67, 101-113.

[27] Zhang Z, Zhang H, Sun W, *et al.* (2022). Optimal energy management of microgrid with hybrid energy storage. *Science Technology and Engineering*, 22(25), 11049-11056.

[28] Samy MM, Mosaad MI, Barakat S. (2021). Optimal economic study of hybrid PV-wind-fuel cell system integrated to unreliable electric utility using hybrid search optimization technique. *International Journal of Hydrogen Energy*, 46(20), 11217-11231.

[29] Das BK, Hoque N, Mandal S, *et al.* (2017). A techno-economic feasibility of a stand-alone hybrid power generation for remote area application in Bangladesh. *Energy*, 134, 775-788.

[30] Diab AAZ, Sultan HM, Mohamed IS, *et al.* (2019). Application of Different Optimization Algorithms for Optimal Sizing of PV/Wind/Diesel/Battery Storage Stand-Alone Hybrid Microgrid. *IEEE Access*, 7, 119223-119245.

[31] Skarstein Ø, Uhlen K. (1989). Design Considerations with Respect to Long-Term Diesel Saving in Wind/Diesel Plants. *Wind Engineering*, 13(2), 72-87.

[32] Zhao Y, Liu Y, Wu Z, *et al.* (2023). Improving Sparrow Search Algorithm for Optimal Operation Planning of Hydrogen–Electric Hybrid Microgrids Considering Demand Response. *Symmetry*, 15(4), 919-941.

[33] Abdalla AN, Nazir MS, Tao H, *et al.* (2021). Integration of energy storage system and renewable energy sources based on artificial intelligence: An overview. *Journal of Energy Storage*, 40, 102811-102823.

[34] Belboul Z, Toual B, Kouzou A, *et al.* (2022). Multiobjective Optimization of a Hybrid PV/Wind/Battery/Diesel Generator System Integrated in Microgrid: A Case Study in Djelfa, Algeria. *Energies*, 15(10), 1-30.

[35] Ma J, Zhang X, Zhang Z, *et al.* (2022). Microgrid Capacity Optimizaiton Based on Improved Sparrow Search Algorithm. *Electronic Measurement Technology*, 45(08), 76-82.

[36] Dong J, Dou Z, Si S, *et al.* (2021). Optimization of capacity configuration of wind–solar–diesel–storage using improved sparrow search algorithm. *Journal of Electrical Engineering & Technology*, 17(1), 1-14.

[37] Lyu Z, Tan Y, Li J, *et al.* (2017). Multi-objective Optimal Sizing for Distributed Generation of Isolated Hybrid Microgrid Using Markov-based Electromagnetism-like Mechanism. *Proceedings of the CSEE* 37(7), 1927-1936.

[38] Liang C, Ding C, Zuo X, *et al.* (2023). Capacity configuration optimization of wind-solar combined power generation system based on improved grasshopper algorithm. *Electric Power Systems Research*, 225, 109770-109782.

[39] Menshsari A, Ghiamy M, Mousavi MM, *et al.* (2013). Optimal design of hybrid water-wind-solar system based on hydrogen storage and evaluation of reliability index of system using ant colony algorithm. *Int. Res. J. Appl. Basic Sci*, 4(11), 3582-3600.

[40] Zhang L, Zheng L, Leng X, *et al.* (2023). Research on Multi-Objective Optimization Strategy of Wind-Photovoltaic-Pumped Storage Combined System Based on Gray Wolf Algorithm. *Journal of Shanghai Jiaotong University*, 1-25.

[41] Islam M, Akter H, Howlader H, *et al.* (2022). Optimal Sizing and Techno-Economic Analysis of Grid-Independent Hybrid Energy System for Sustained Rural Electrification in Developing Countries: A Case Study in Bangladesh. *Energies*, 15(17), 6381-6402.

[42] Guneser MT, Elbaz A, Seker C. (2022). Hybrid Optimization Methods Application on Sizing and Solving the Economic Dispatch Problems of Hybrid Renewable Power Systems. In M. A. Mellal (Ed.), *Applications of Nature-Inspired Computing in Renewable Energy Systems* (pp. 136-165). Hershey, PA, USA: IGI Global.

[43] Mirjalili S, Mirjalili SM, Lewis A. (2014). Grey Wolf Optimizer. *Advances in Engineering Software*, 69, 46-61.